Cytochrome b_{562} Variants: A Library for Examining Redox Potential Evolution†

Stacy L. Springs, Susanna E. Bass, and George L. McLendon*

Department of Chemistry, Princeton University, Princeton, New Jersey 08544

Received January 28, 2000; Revised Manuscript Received March 7, 2000

ABSTRACT: A general understanding of how cytochromes evolve within a fixed structure to optimize redox potential for specific bioenergetic processes does not exist. Toward this end, a library approach is used to investigate the range and distribution of redox potential which occurs when all sequence space available through mutation at two positions is examined within a fixed structural motif. Random mutation of Phe61 and Phe65 of cytochrome b_{562} (*E. coli*), and subsequent examination of a statistically significant sampling of this library, demonstrates that the redox potential can vary over 100 mV (>25% of the known accessible potential in native proteins with axial His-Met ligation) through mutation at these two positions. The redox potential of the wild-type protein occurs at an extremum of the distribution observed, indicating that Phe61 and Phe65 were most likely naturally selected to differentially stabilize the reduced state of the protein. At the other extremum, a compositionally conservative set of mutations (F61I, F65Y) leads to a 100 mV shift in the redox equilibrium toward the oxidized state. NMR analyses indicate that a charge-dipole interaction which results from mutation of phenylalanine to tyrosine at position 65 may be responsible.

The reactivity and associated function of electron transfer proteins depends critically on the redox potential of the protein. The midpoint redox potentials exhibited by the *b*- and *c*-type cytochromes vary between −400 and 400 mV vs NHE, a range which highlights the profound importance of the "tunability" of redox potential by the surrounding protein in carrying out a wide variety of bioenergetic processes (*1, 2*). Evolution has generated a broad spectrum of redox potentials among the cytochromes; however, we still neither have a general ability to predict redox potential for a given structure nor understand the range of potential which can be accessed via evolutionary (mutagenic) variation within a fixed overall structural motif. In this manuscript, we outline an approach to understanding such unknowns, wherein a small, soluble cytochrome (cytochrome b_{562}) is used to investigate the range of redox potential which can be accessed by random mutation at two positions while holding the overall folding pattern fixed.

While certain classes of native cytochromes (i.e., *c*-type) exhibit similar folds, they also have nonnegligible structural differences such as additional or missing surface loops (or helices), as well as differences in the charge present at the exposed heme edge, and often a marked lack of sequence homology (*3*). Therefore, any conclusions about range and distribution of redox potential within such a "structural" class of existing proteins would necessarily have to assume that these differences are not important to the definition of redox potential. As this seems presumptuous, a different approach might be to examine redox variants where the wild-type and variant proteins are identical other than a few residues which have been mutated. Only a few sets of redox variants with this degree of structural homology [i.e., cyt *c* (*4*−*9*), cyt b_5 (*8*−*10*) variants] exist, and the range of redox potential exhibited in these families is relatively small. For instance, if one considers the redox potentials for double mutants of cytochrome *c* (not including mutation to the axial ligands), a range of 82 mV of potential has been observed (*4*). Of course, these families have only included variants in which one or two amino acid substitutions were considered at any particular position. Thus, it remains open to speculation what range of potential can be generated within a set of structurally similar cytochromes through mutation at an individual position or set of positions. Perhaps a wide range of redox potential is available within a structural motif through mutation in the local environment of the heme, but the right "set" of mutations has not been chosen to demonstrate this effect. Further, because self-compensating synergistic effects frequently occur (*4*), the probability of "hand-picking" a redox variant with both nativelike stability and a specified potential is greatly diminished when two or more residues are mutated simultaneously. Moreover, this approach gives essentially 1 datum per experiment, and thus addresses neither the question of what range of redox potential is possible (in the event that an amino acid residue is allowed to vary for all 20 naturally occurring amino acids) nor what the distribution within this range will be. In other words, a point mutation may result in a dramatic shift in redox potential; however, an understanding of where that shifted potential lies among all possible potentials available through all mutations at this position cannot be gained in this way. Thus, to investigate the range and distribution of redox potentials which can be produced in a series of mutants which maintain a large degree of both structural and sequence homology, a first-generation library of cytochrome b_{562} mutants was prepared, and the midpoint redox potentials of a statistical sampling of this library were determined.

† This work was supported by the NIH (GM18627-02 and GM33881).

* To whom correspondence should be addressed.

10.1021/bi0001675 CCC: $19.00
Published on Web 04/26/2000

Cytochrome b_{562} is a small, soluble, redox-active protein, isolated from the periplasm of *E. coli*. It is thought to be an electron transport protein although its exact function remains unknown. The crystal structure of ferricytochrome b_{562} has been solved at 1.4 Å resolution (*13*), and the solution structure of the oxidized holoprotein has also recently been solved (*14*). These structures describe four α-helices connected by three turns to form a left-handed supercoiled helix bundle. A noncovalently bound heme is found near the C and N termini, the 6-coordinate iron group of which is ligated to Met7 and His102. Cytochrome b_{562} is an ideal candidate for this study because (a) it can easily be overexpressed in *E. coli*, (b) it is small (12.3 kDa) and therefore the native and mutant proteins are amenable to NMR analysis, and (c) it contains a noncovalently bound heme which becomes important in the screening process, in which a color assay is used to pick cells which overexpress *properly folded* mutants which have also maintained a significant affinity for the *b*-type heme of cyt b_{562}. *E. coli* containing mutants which bind heme are red in color and easily detectable (*15*), while those that have not folded properly, or the active sites of which have been perturbed to the extent that heme binding is not possible, remain colorless. Thus, the screen is based on structural rather than functional criteria, since structural criteria allow expression of the full range of (stable) heme-binding mutants, while natural selection necessarily precludes redox extrema which cannot maintain function in vivo.

EXPERIMENTAL PROCEDURES

Cloning and Mutagenesis. Cytochrome b_{562} was expressed under *lac* control using a pEMBL18-based plasmid (pRW1) which contains the entire cyb C gene and native periplasmic signal sequence (*15*). Combinatorial cassette mutagenesis, specifically overlap−extension PCR-based mutagenesis (*16, 17*), was used to generate a library of dsDNA containing randomization at the codons corresponding to Phe61 and Phe65. The procedure described by Kadowaki et al. was modified from single-base variation for the introduction of randomization at two codons. Two PCR reactions utilizing oligonucleotide primers (OEP1B and OEP2) and (OEP3 and OEP4B) were used to generate two pieces of DNA which have a region of terminal complimentary. The oligonucleotides used were the following: OEP1B, 5′-BIOTIN-CGCGCAGAATTCGAGCTCGGTACCCGGGCGAAT-3′; OEP2, 5′-ATCTTTCATTTCCGGGCTGTCCGGTG-3′; OEP3, 5′-GACAGCCCGGAAATGAAAGATNNSCGCCACGGTNNSGACATTCTGGTCGGTCAGATTGAC-3′; OEP4B, 5′-BIOTIN-CGCGGCGGATCCCGACGGCAAATTTGTGCAG-3′. Oligonucleotides OEP1B and OEP4B also contain restriction enzyme sites flanked by several additional bases at their 5′ ends (*Eco*RI and *Bam*HI). Subsequently, the products of these two reactions (one of which contains the randomization) are spliced together using a PCR-based extension and the products subsequently amplified. The PCR product corresponds to the entire length of the cyb C gene. The PCR product was digested with *Eco*RI and *Bam*HI restriction enzymes, and the dsDNA library was introduced into the vector pRW2 (identical to pRW1, except that the cyb C gene contains a frameshift and deletions which result in proteolytic degradation). The dsDNA library was cloned into vector pRW2 to prevent any positive background in the color screening process which might arise from uncut plasmid if pRW1 were used as the vector. The recombinant plasmid library was transformed into *E. coli* strain MV1190 by electroporation. The *E. coli* was grown on 2 × YT plates with 100 μg/mL ampicillin. Individual colonies were transferred to 3 mL of 2 × YT with 100 μg/mL ampicillin and grown at 37 °C to an OD of ∼1.0. The cells were then induced with 100 μg/mL isopropyl-1-thio-β-D-galactoside and shaken at 250 rpm for 18 h. The cells were harvested by centrifugation and examined for enhanced pink or red color relative to a negative control (*E. coli* strain MV1190 bearing plasmid pRW2).

Protein Purification. The isolation and purification of the wild-type and mutant proteins was achieved by a freeze−thaw lysis to remove the contents of the periplasm as previously described (*15*). The pH of the supernatant was adjusted to 4.2 using 1 M sodium acetate buffer. After 1 h at 4 °C, the precipitated protein impurities were removed by centrifugation. The supernatant was concentrated and subjected to size exclusion chromatography on a Superdex 30 column equilibrated with 20 mM potassium phosphate buffer (pH 7.4), 150 mM NaCl. The eluted protein was buffer-exchanged into 20 mM potassium phosphate buffer (pH 7.4), and purified by anion exchange on a Mono Q column. The holoprotein was eluted using a gradient of 0−0.5 M NaCl. In some cases, the purification was completed on an SP Sepharose FF column. In these cases, the purification was carried out in 50 mM sodium acetate buffer (pH 4.5), and the proteins were eluted with a gradient of 0−0.5 M NaCl. The proteins used spectroelectrochemical studies and were purified to an absorbance ratio A_{418}/A_{280} of 5.7 or higher and assessed to be greater than 90% pure by SDS−PAGE analysis. The integrity of all mutants was confirmed by electrospray ionization mass spectrometry on a Hewlett-Packard 5989B mass spectrometer and DNA sequencing analysis on an ABI PRISM 377 Sequencer.

Spectroelectrochemistry. The spectroelectrochemical titrations were performed under anaerobic conditions in a cell constructed with 1.5 in. × 2 in. × 2.25 in. piece of Lexan, two quartz windows, an optically transparent thin-layer electrode (gold minigrid, 500 lines in.$^{-1}$; Buckbee-Mears Co.) as the working electrode, a platinum wire counter-electrode, and a Ag/AgCl reference electrode (BAS) which was isolated from the sample compartment by a Luggin capillary. The spectroelectrochemistry was performed using a Perkin-Elmer Lambda 6 UV/Vis spectrophotometer and a Cypress Systems Model CS-1090 Potentiostat. The proteins were buffer-exchanged using a PD-10 column into 20 mM potassium phosphate buffer (pH 7.2), 100 mM NaCl. The protein samples with mediator [ethylenediaminetetraacetic acid, iron(III) sodium salt ($E°$ vs NHE = 120 mV), or 2,3,5,6-tetramethylphenylenediamine ($E°$ vs NHE = 260 mV)] present were flushed with nitrogen prior to introduction into the spectroelectrochemical cell. The protein concentrations were approximately 5×10^{-5} M, and the mediator concentrations were between 0.5×10^{-3} and 1.0×10^{-3} M. The protein/mediator sample was introduced into the cell via syringe and the sample equilibrated at −600 mV for approximately 20 min to reduce any residual oxygen in the sample. The absorbance at the characteristic 562 nm band of cytochrome b_{562} was recorded after equilibration at several potentials between −600 and 200 mV. The data were fit to the one-electron Nernst equation and evaluated at 29 °C.

NMR Spectroscopy. The wild-type protein and the (Phe61Ile, Phe65Tyr) mutant were dialyzed into 0.5 M phosphate buffer in 99% D_2O. The phosphate buffer was prepared from deuterated phosphoric acid and sodium deuterooxide. The pH* of the buffer was 7.1, a value which is not corrected for the deuterium isotope effect. The oxidized and the reduced proteins were analyzed at concentrations of 1.3 and 1.5 mM for the wild type and mutant, respectively. The reduced spectra were collected in the presence of 10 mM sodium dithionite. The solutions were purged with nitrogen prior to addition of dithionite and then capped for the duration of the experiment. All NMR experiments were run on a Varian Unity/INOVA (Varian, Palo Alto,CA) 600 MHz spectrometer at 25 °C. For data processing and visualization of 1D spectra, Vnmr software (Varian) was used, while 2D data were processed in NMRPipe (*18*), and visualized and analyzed in NMRView (*19*). One-dimensional ^1H experiments of the oxidized WT and mutant samples were done in D_2O using a 50 kHz spectral window and a short enough (ca. 5°) read pulse to cover the whole frequency range of interest. Typical parameters were 64K total number of acquired data points and processing with 1 time of zero-filling and exponential line broadening of 5−20 Hz. One-dimensional spectra of the reduced derivatives were acquired with a 12K spectral window and processed the same way. Two-dimensional NOESY (w/100 ms mixing time) spectra were acquired with 4096* points in $t2$ and 2 × 512 $t1$ increments, using States−Redfield (*20*) phase cycling for sign discrimination. Processing included apodization with a combination of shifted cosine bell and Gaussian functions and baseline correction in both dimensions both by linear interpolation and by polynomial fit. The final size, after zero-fills in both dimensions, was 8K × 2K points. Gradient-elected magnitude mode 2Q-HoMQC spectra (*21*) (with 30 ms excitation delay) to map through-bond connectivities were acquired with the same parameters.

RESULTS

Library Design. To create a library of cyt b_{562} mutants in which the overall fold is identical to the wild-type protein, while maintaining a high probability of revealing a large range of redox potential, cassette-mediated mutagenesis was used to simultaneously randomize positions corresponding to 2 residues for all 20 naturally occurring amino acids in the region near the heme of cytochrome b_{562}. To ensure that a statistical analysis would give meaningful results, the randomization was kept at a maximum of two positions per generation of library. In this way, the maximum possible library size is limited to 400 members, so that one need only sample ca. 15 members to ensure with high confidence levels that the range of redox potential observed corresponds to the range existing in the entire population (*22*). The results of the first generation of this library are presented here.

The mutagenesis strategy involves the randomization of codons corresponding to amino acid residues Phe61 and Phe65 which form a hydrophobic pocket surrounding pyrrole ring C of the heme (Figure 1). Phe65 is almost parallel with the heme and in van der Waals contact with the vinyl β substituent of pyrrole ring C on the face which is adjacent to Met7, while the aromatic planes of Phe61 and the heme lie perpendicular to each other (*13*). An NNS (N equals an equimolar mixture of A, C, G, and T; and S equals an equimolar mixture of G and C) randomization was used at positions 61 and 65. The DNA from each positive clone (i.e., red *E. coli*) was sequenced using standard dideoxynucleotide-sequencing techniques. Proteins panned from *E. coli* cultures during the color screen were purified according to the protocol outlined under Experimental Procedures, and the expected mass was confirmed by electrospray mass spectrometry. The identities of 29 variants which were randomly chosen from colonies exhibiting a pink or red color are given in Table 1.

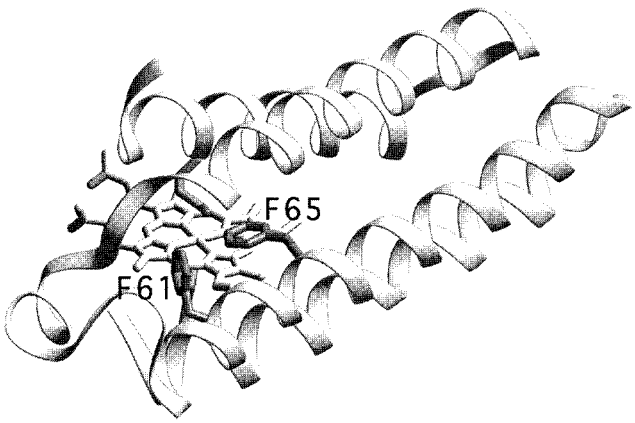

FIGURE 1: Ribbon representation of the crystal structure of ferricytochrome b_{562} with the heme, the Met7 and His102 axial ligands, and the two sites of mutation (Phe61 and Phe65) highlighted.

Table 1: Nucleotide and Amino Acid Sequences of 29 Members of the Cytochrome b_{562} Library Randomly Chosen Using a Color Screen for Properly Folded, Heme Binding Variants

nucleotide sequence		amino acid sequence	
Pos 61	Pos 65	Pos 61	Pos 65
GCC	TTC	Ala	Phe
GGG	TTC	Gly	Phe
TTC	GTG	Phe	Val
TGG	TCG	Trp	Ser
TGG	TGC	Trp	Cys
TGG	CAC	Trp	His
GCG	TTG	Ala	Met
GCG	TTG	Ala	Leu
TTG	TTG	Leu	Leu
GTC	TTG	Val	Leu
CTG	ATC	Leu	Ile
GTG	ATC	Val	Ile
ATG	TGG	Met	Trp
ATC	TAC	Ile	Tyr
TGC	TTG	Cys	Leu
ACG	TGC	Thr	Cys
TGG	CTC	Trp	Leu
TGG	GGG	Trp	Gly
TGG	ACG	Trp	Thr
GGC	TTG	Gly	Leu
TGG	TGG	Trp	Trp
GGC	GTG	Gly	Val
TCG	TTC	Ser	Phe
GTC	AAG	Val	Lys
ATG	CTC	Met	Leu
TTC	GCC	Phe	Ala
GTG	ATC	Val	Ile
TGG	CTG	Trp	Leu
TCC	GCC	Ser	Ala

Sequencing Analysis. The diversity of the library at the genetic level was determined by DNA sequencing of 60 clones prior to library screening. The expected nucleotide

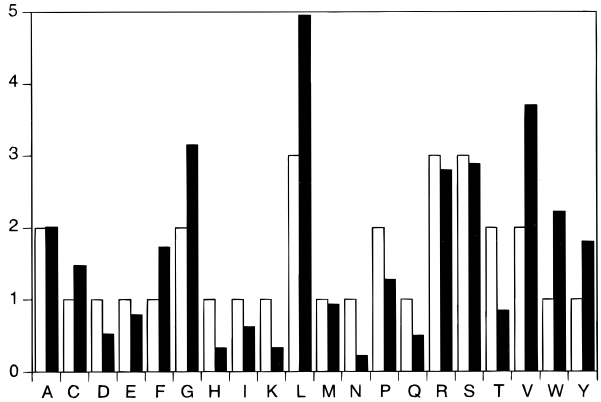

FIGURE 2: Expected amino acid distribution in an unbiased NNS randomized library (□, where N = equimolar G, A, C, T; and S = equimolar G and C) and in the biased NNS library as determined by sequencing analysis (■).

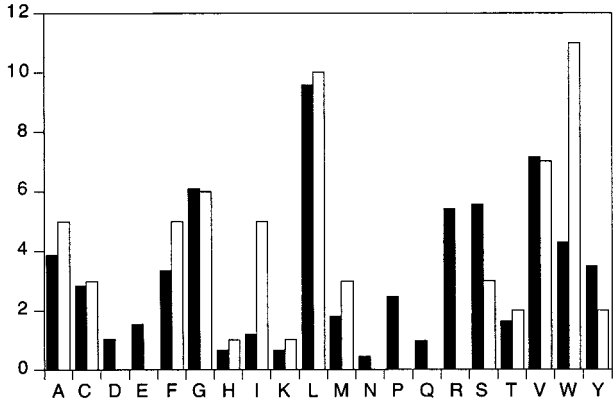

FIGURE 3: Expected amino acid distribution based on sequencing data (■) and the observed amino acid distribution in library members selected on the basis of red phenotype (□).

frequency at N positions is 25% G, A, C, and T; while the expected nucleotide frequency at S positions is 50% G and 50% C. The actual frequencies were found to differ at N positions with G and T overrepresented (37% and 31%, respectively), and A and C underrepresented (18% and 14%). At S positions, C was present 37% of the time, while G was present 67% of the time. Such bias can originate at the solid-phase oligonucleotide synthesis level or as a result of selection at the DNA synthesis level during the polymerase chain reaction. This type of bias is common in combinatorial cassette mutagenesis where random oligonucleotide primers, enzymatic second-strand synthesis, or inosine pairing is used (*17*, *23*). Fortunately, this bias can be assessed. The expected occurrence of amino acids in the library based on the observed nucleotide frequencies is shown in Figure 2. Also shown in Figure 2 is the expected occurrence of amino acids in a library based on an NNS randomizaton which only contains the bias inherent in the genetic code. Figure 2 shows that while the representation of some amino acids has diminished, no amino acids have a probability of occurrence approaching zero relative to the other amino acids. Therefore, it is likely that all 400 library members are represented at the genetic level. Of the 60 clones sequenced, 30 contain frameshift or bonus mutations, while 30 contain desired mutations only. Importantly, the distribution of nucleotides at the N and S positions does not change if one compares only the 30 sequences without frameshift mutations to all 60 sequences analyzed. Thus, it is unlikely that certain sequences predispose the polymerase toward deletions or insertions. Of the 30 viable sequences, 17 produced red *E. coli* and 13 produced white *E. coli*. Two of the white *E. coli* contain sequences where stop codons have been introduced. The remaining 11 either do not bind heme or do not fold properly, or a combination of both in vivo. SDS−PAGE analysis shows that the presence of apocytochrome b_{562} variants in bacteria which were negative during the color screen was diminished or absent entirely following freeze−thaw lysis. One possible explanation for this is that heme binding may be a prerequisite for in vivo stability of cytochrome b_{562} and variants.

Residue Types. In Table 1, 29 unique variants which exhibit a red phenotype in the color screen are listed. The last 15 of these are positive clones described in the sequencing analysis. The first 14 are from an analogous phenotypic screen from the same plasmid library pool. Duplicate sequences (three at the amino acid level) were removed from the list for conciseness (however, they were included in the distributions shown in Figure 3). A comparison of the amino acid distribution expected (based on our sequencing analysis) and the amino acid distribution observed after screening (based on red phenotype) is shown in Figure 3. Examination of Figure 3 shows that the hydrophobic residues L and V are normally represented, while the other hydrophobic residues (F, M, and especially I and W) are overrepresented. The residues A, C, and G are normally represented, while S and Y are slightly underrepresented. D, E, N, P, Q, and R do not occur. In the case of D, E, N, and Q, the expected occurrence and sample size are too small to allow any statement to be made about the absence of these residues. However, in the case of P and particularly R (not present after the color screen despite its predicted occurrence 5 times), the data suggest that the folded, heme-bound state of variants containing these two residues may not be not stable.

UV//Visible Absorbance Spectroscopy. The absorbance spectra of hemoproteins are very sensitive to perturbations of the electronic environment around the heme. Therefore, a comparison of the visible absorbance spectra of wild-type cytochrome b_{562} and the cytochrome b_{562} mutants allows, to a first approximation, a probe of the structural integrity of the heme pocket. All mutants except one exhibit identical absorbance spectra to those of the wild-type protein in both the reduced and the oxidized state. However, in the case of the (Phe61Trp, Phe65His) variant, while the absorbance spectrum of the ferrocytochrome is unperturbed, the Soret band of the ferricytochrome mutant is blue-shifted by 6 nm. This indicates that in the oxidized state, the heme environment has been perturbed, possibly reflecting a redox-linked conformational change for this mutant. If such a conformational change does exist, the redox potential measured by the equilibrium methods described could reflect a combination of redox potentials in each conformation.

Redox Potentials. The midpoint redox potentials of wild-type cytochrome b_{562} and 14 mutants were determined using spectroelectrochemistry. An overlay of the absorbance spectra at several applied potentials during a spectroelectrochemical titration of wild type b_{562} is given in Figure 4. In the presence of DAD (2,3,5,6-tetramethyl-1,4-phenylenediamine), the protein is interconverted from ferro- to ferri-cytochrome b_{562}

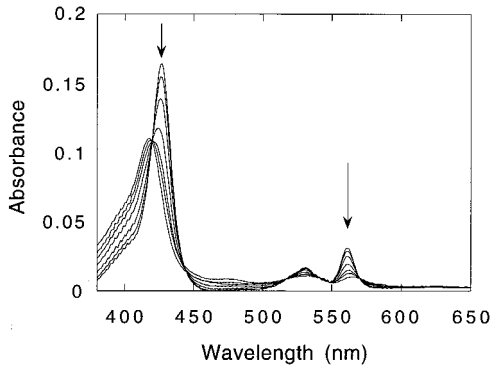

FIGURE 4: Overlay of the visible absorbance spectra of wild-type cytochrome b_{562} at several applied potentials (−500 to 100 mV) during a spectroelectrochemical titration in the presence of the mediator DAD. The arrows indicate the conversion from ferro- to ferricytochrome b_{562}.

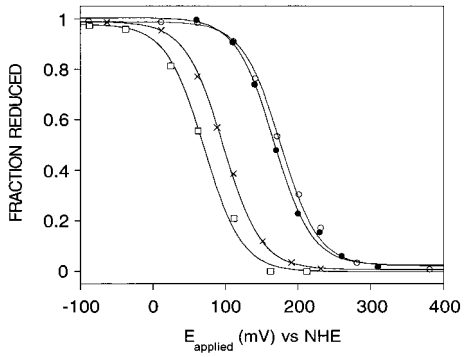

FIGURE 5: Raw data and nonlinear least-squares curve fits to the one-electron Nernst equation for the spectroelectrochemical reduction of (○) F65V, (●) wild-type cytochrome b_{562}, (×) F61G, and (□) F61I, F65Y. The associated midpoint redox potentials are 173, 168, 96, and 68 mV vs NHE.

with an absorbance profile exhibiting clean isosbestic points. This profile is also observed in the data for the mutants described in this study. Figure 5 shows the raw data and nonlinear least-squares curve fits to the one-electron Nernst equation for the WT protein and several representative mutants. The error associated with these measurements is estimated to be approximately ±5 mV based on variation between different titrations of the same protein. The values determined correspond well to what has been previously measured by both direct electrochemical (*24*) and potentiometric methods (*25*) when compared at the same pH (7.2) and when the temperature dependence of the redox potential is considered. The midpoint redox potentials for wild-type cytochrome b_{562} and 14 mutants are given in Figure 6.

The range exhibited by this first-generation library is 105 mV, a range which is significant when one considers that neither of the axial ligands have been altered and only 2 of 15 possible residues which are in van der Waals contact with the heme of the wild-type protein have been altered in this round of mutagenesis. Interestingly, all mutations except one (Phe65Val) result in proteins which are more easily oxidized (or less easily reduced) than the wild-type protein (Figure 6). A further examination of the distribution shows that the majority (>70%) of the mutations result in relatively small shifts in potential of 45 mV or less. Still, approximately 30% (4 mutants) display redox potentials which are shifted by 55 mV or more. The variant with the furthest shifted potential (F61I, F65Y) clearly exemplifies that the mutations which

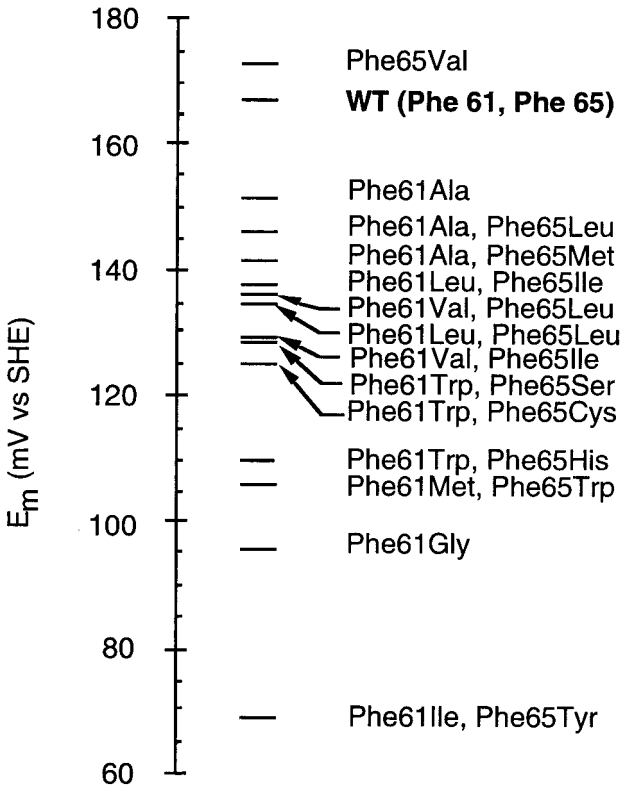

FIGURE 6: Range of midpoint redox potential exhibited by a statistical sampling of a first-generation library of cytochrome b_{562} variants. The wild-type potential is shown in boldface type and occurs at an extremum of the distribution. The error associated with these measurements is ±5 mV.

led to this, the most dramatic effect, were neither predicted nor expected. In the case of (F61I, F65Y), differences in overall accessible surface area and side chain volumes for the two residues which replace Phe61 and Phe65 are minimal, yet a 100 mV shift in potential is observed (E_m = 68 mV vs NHE). Further, in the absence of major changes to the heme pocket topology, it is unlikely that the solvent exposure of the heme could be significantly increased through these mutations.

While the primary focus of this work is to examine the range and distribution of the library of redox variants described herein, it also is of interest to understand why (F61I, F65Y) exhibits such a dramatic shift in redox potential relative to the wild-type protein. The proximity of the tyrosine 65 hydroxyl group to the iron atom of the heme was considered a possible explanation for the generation of such a large shift in potential. We considered that the oxidized state of the mutant could be stabilized through either a direct electrostatic stabilization between deprotonated Y65 and Fe(III) or a charge-dipole interaction between protonated Y65 and Fe(III) (*26*). First, it was necessary to rule out the possibility that in the (F61I, F65Y) mutant, the pK_a of the tyrosine phenolic proton might be altered to the extent that at pH 7.2 it is predominantly deprotonated. If this were in fact true, a direct electrostatic interaction between Fe(III) and Y65(OH) might occur. If Y65 is deprotonated at pH 7.2, it should be reflected in the pH dependence of the midpoint redox potential. The midpoint redox potential of wild-type cytochrome b_{562} has been examined and exhibits a marked pH dependence with at least three titratable groups (*24, 25*). Any marked deviation from the pH dependence

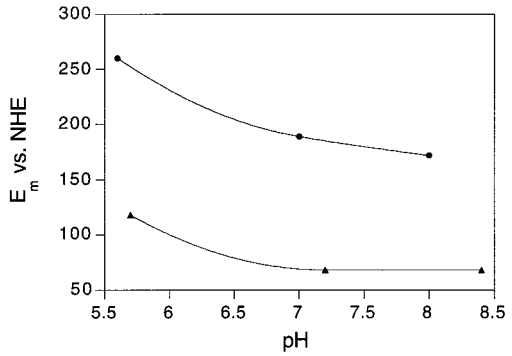

FIGURE 7: pH dependence of the midpoint redox potential of the F61I, F65Y variant (▲) recorded in 20 mM phosphate buffer, 100 mM NaCl. The values for the wild-type protein (●) were taken from Barker et al. (*24*).

($\delta E/\delta$pH) observed in the case of the wild-type protein might indicate that the tyrosine OH ionizes within the pH range under study. However, as can be seen in Figure 7, no substantial deviation is observed, which means that under the conditions of these experiments ($5.5 < pH < 8.5$), Y65 does not change protonation state. It is unlikely that the pK_a of the tyrosine OH would be altered to the extent that it would not be substantially protonated at pH 5.5 (normal pK_a of the tyrosine side chain proton is 10.5). Therefore, we suggest that tyrosine 65 is protonated under the conditions that the redox potential was measured (pH 7.2).

NMR Experiments. Under these circumstances, we envisioned two possible explanations for a 100 mV shift in redox potential. The first is that, as a result of these mutations, the structure has *not* remained that same. The second explanation invokes a charge-dipole effect which would arise as a consequence of the proximity of tyrosine 65 to Fe(III) and result in the stabilization of the oxidized protein. Using NMR spectroscopic measurements of the reduced wild-type and variant proteins, we sought to rule out the possibility that a gross structural change, the first of these possibilities, might be responsible. Further, if the structural integrity of this mutant has been maintained, a spectral analysis might also allow us to glean why, in what is a structurally conservative set of mutations, such a dramatic shift in potential results.

All of the heme resonances of cytochrome b_{562} in the reduced state, as well as resonances belonging to the four aromatic residues in the heme pocket (Phe61, Phe65, Tyr101, and Tyr105), have been previously assigned (*27*). With these assignments in hand, a comparison of wild-type and mutant NOE's corresponding to through-space interactions in the region of the heme allows assessment of whether the overall structure of the mutant has been perturbed.

In cytochrome b_{562}, there is direct evidence for heme orientational disorder, where an isomer in which a 180° rotation about the $\alpha-\gamma$ meso axis of the heme has occurred, and accounts for approximately 15−30% of the species in solution (*14, 27, 28*). Under the conditions of the experiments described herein, a second set of resonances are also observed in the spectra of the wild-type protein and correspond to the previously described minor isomer. Similarly, both major and minor isomers of the (F61I, F65Y) variant are also observed. A comparison of the chemical shifts and the NOE patterns of resonances corresponding to heme substituents and conserved aromatic residues (i.e., Y101, Y105) in the heme pocket provides an indication that the region surrounding the heme has not been perturbed through replacement of Phe61 and Phe65 with Ile61 and Tyr65 (see Table 2). This provides evidence that the *overall* topology of the heme pocket is conserved in the wild-type and mutant proteins. Further, the resonances previously assigned to F61 and F65 are observed in the wild-type spectra but not in the mutant (see Figure 8). Conversely, a new set of aromatic resonances at 5.95 and 6.90 ppm are observed in the spectra of the variant and are thereby assigned to the (3, 5) and (2, 6) protons of Y65, respectively (see Figure 8c,d). In the NOE spectrum of the wild-type protein, the presence of a strong NOE between the axial ligand Met7 $C_\epsilon H_3$ protons and the F65 (4) and (3, 5) protons establishes the proximity of this residue to Met7 and the iron center. In the variant, the presence of a strong NOE between the Y65 (3, 5) protons and the Met7 methyl protons (−3.06 ppm) and a weak NOE between the Y65 (2, 6) protons and Met7 methyl protons indicates that, like F65 which it replaced, the (3, 5) protons of Y65 are within 4 Å of the Met7 methyl group (see Figure 8). These data indicate that the overall topology of the heme crevice is similar to that found in wild-type cytochrome b_{562} and that the tyrosine residue is, within the limitations of this experiment, in the same position as the phenylalanine which it replaced. It certainly establishes the proximity of this residue to the redox center and implies that a charge-dipole interaction between Fe^{3+} and Tyr65 is a likely explanation for the observation of a dramatic shift in the midpoint redox potential of this mutant relative to the wild-type protein. As mentioned previously, the solution structure of ferricytochrome b_{562} has recently been solved (*14*). While, in principle, this should allow detailed information about the oxidized state of the variant to be obtained, analysis of such spectra is necessarily more complicated. This is because the spectrum of oxidized ferricytochrome b_{562} exhibits a large degree of spectral overlap, and therefore, only some of the aromatic resonances (of the major isomer only) have been assigned by Arnesano et al. In light of this, a more detailed analysis is required for assignment of the aromatic region of the variant, and these results will be reported in due course.

Table 2: Assignments for Selected Aromatic Residues of Ferrocytochrome b_{562} and the F61I, F65Y Variant

	wild-type major isomer (*24*)	wild-type major isomer (this study)	F61I, F65Y major isomer (this study)
F61 (4)	7.27	7.25	−
F61 (2,6)	7.49	7.44	−
F61 (3,5)	8.04	8.00	−
F65 (4)	5.5	5.42	−
F65 (2,6)	6.80	6.71	−
F65 (3,5)	5.76	5.70	−
Y101 (2,6)	7.67/7.62	7.58	7.56
Y101 (3,5)	7.14	7.06	6.92
Y105 (2,6)	7.67/7.62	7.58	7.56
Y105 (3,5)	7.14	7.06	6.92
Y65 (2,6)	−	−	6.90
Y65 (3,5)	−	−	5.95
M7 Me	−3.02	−3.09	−3.06

DISCUSSION

We have generated a library of cytochrome b_{562} variants and examined the redox potentials of a statistical sampling of this library. For a statistical analysis, the sample data need to be corrected for bias in the population. An intrinsic bias is introduced by the differing codon frequencies, but ad-

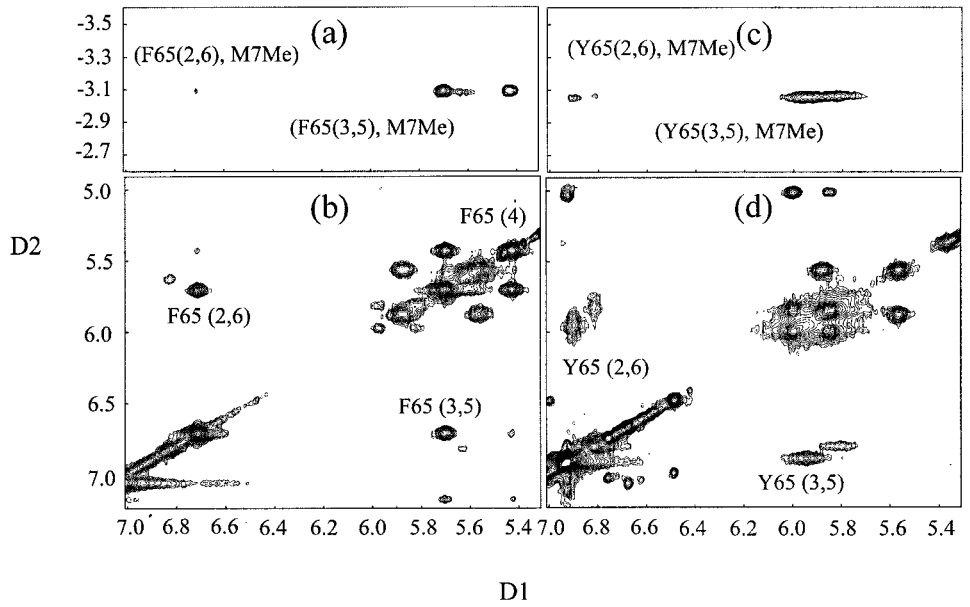

FIGURE 8: Sections of the ^{1}H-NOESY spectra of wild-type cytochrome b_{562} and the F61I, F65Y variant. The spectra were recorded at 25 °C in deuterated sodium phosphate buffer (pH* 7.2) in the presence of 10 mM sodium dithionite. (a) NOE's between the M7 methyl protons and residue F65 protons of wild-type cytochrome b_{562}. (b) Strong NOE's between the F65(2,6) and (3,5) protons of wt b_{562}. (c) NOE's between the M7 methyl protons and Y65 protons of the F61I, F65Y variant. (d) NOE's between the Y65 (2,6) and (3,5) protons of the F61I, F65Y variant.

ditional bias is introduced by the mutagenesis procedures. Such bias, since it can be independently assessed, can be corrected by probability weighting the sample to estimate the mean, the variance, and the range (*29*). For instance, while the unweighted mean is 130 mV, the probability weighted mean is 127 mV. An estimation of the range is more complex. The most conservative possible estimate is given by Chebyshev's theorem (*22*) which makes no assumption about the form of the distribution. By this estimate, the sample data reported here represent at least 75% of the total possible range for the population. For a near normal distribution, using a correctly weighted sample, the range examined corresponds to the range of the entire library (400 possible members) with confidence limits of >90%.

The redox potential of hemoproteins with the same axial ligands can be found to vary by approximately 400 mV (*1, 2, 26*). The first-generation library of b_{562} mutants exhibits a range of 105 mV. This means that through mutation of only two residues, greater than 25% of the known potential possible has been accounted for in this library.

In this library, certain variants which may not bind heme in vivo, might be coaxed into binding heme in vitro, under alternative solution conditions. If such variants exist, they will not have been selected as part of this study, even though they may have interesting redox potentials. In due course, such variants may be isolated as apoprotein and reconstituted with heme, and the redox potential determined. However, in the evolutionary context in which the current results are considered, variants which do not bind heme in vivo are presumably of no use to the organism and irrelevant.

In general, it has been accepted that mutations which only result in changes to the local environment around the heme lead to small perturbations of redox potential, while mutations which lead to new (or disrupt existing) hydrogen bonds to the heme or heme axial ligands, or alter the axial ligands frequently result in large shifts in redox potential (*1*). As the distribution of this range shows, a 100 mV change in potential (as observed in variant F61I, F65Y) is an extremum of the observed potentials. Thus, our results support the idea that local effects can be dramatic, albeit infrequent and not always qualitatively predictable.

Other determinants of redox potential, such as protein tertiary structural differences, have been implicated as a dominating force in the control of redox potential, while, as mentioned, local effects have been considered a determinant of lesser importance (*1*). However, whether the accessible range of redox potential in hemoproteins *is* dominated by such differences has not been determined experimentally. In a similar vein, the hypothesis that solvent exposure of the heme is the dominating factor has been reinvestigated recently in a comparison of different *c*-type cytochromes from various species (*30*). By imposing a correction for axial ligation effects, it has been suggested that solvent exposure of the heme can account for over 500 mV of range in potential among *c*-type cytochromes. However, while the proteins in this study maintain a certain degree of structural homology, they also contain nonnegligible differences, suggesting that, in the absence of a full consideration of all energetic contributions from other factors which are known to be important, such a conclusion should be regarded carefully. A contraindication is found in structurally conservative mutations which result in dramatic changes in redox potential as found in mutant (F61I, F65Y). Whether or not the range of accessible potential could be expanded to include the approximately 400−500 mV of known "redox potential space" for cytochromes with His-Met ligation without dramatically changing the solvent exposure of the heme is uncertain, but given the current data, it is a possibility that should not be ruled out.

It is noteworthy that the overall distribution of redox potential is shifted to lower potentials than wild type in all cases except one; in other words, most mutations result in proteins which are more easily oxidized than is the wild-type protein. The mean of the distribution is 127 mV, which

reveals that the potential of the wild-type protein is at an extremum of this distribution. The probability that the redox potential of wild-type cyt b_{562} would occur at this place in the distribution by chance is less than 7%. This suggests that Phe61 and Phe65 were most likely "naturally selected" to differentially stabilize the reduced form of the protein (insofar as it is true that cytochrome b_{562} functions as an electron transport protein). Such a result is not necessarily intuitive, since cytochromes with His-Met coordination exhibit a wide range of potential (ca. 400 mV) and b_{562} lies near the midpoint of that range. One might equally envision evolutionary pressures to differentially stabilize an oxidized redox state, or even to "buffer" the redox state against mutational variations within a given geometry. However, when we examine b_{562} alone, it becomes clear that the wild-type value is anomalous among all the possible potentials accessible through mutations at positions 61 and 65. Furthermore, this result is not unique. For example, an array of mutations in cytochrome *c* have been examined in which synergistic effects occur (*4*−*6*). Again, virtually every mutation or set of mutations shifts the redox equilibrium toward the oxidized state. Thus, cytochrome *c* may also represent an extremum in redox potential. However, in the case of cytochrome *c*, the redox potential has been examined for mutations made at many positions, rather than sampling all possible mutations at two distinct positions. Therefore, while it is not possible to say that a particular amino acid at a particular position has been "naturally selected" to stabilize the reduced form of the protein, it is nevertheless striking that the redox potentials of mutants on hand suggest that this might be so.

CONCLUSIONS

Library techniques have been applied to investigate the range of redox potential which can be accessed through limited internal mutations which preserve the overall fold in cytochrome b_{562}. We find that of the total range of 400 mV observed for cytochromes with fixed Met-His ligation, the conservative mutation of only two residues in b_{562} allows one to access over 100 mV, or 25% of the total (possible) range. Statistical analysis suggests that the 105 mV range found in 15 library members represents with >90% confidence, the total range possible for all mutations at these positions. Finally, examination of the range suggests that the wild-type value is itself "anomalous", being situated at the high potential extreme. Examples from other cytochromes suggest that this may be a common phenomenon, although the available data are not amenable to rigorous statistical analysis. Perhaps many cytochromes evolve to stabilize the reduced state insofar as possible within a fixed topology (which governs associated recognition and electron tunneling reactivity). This suggests an underlying strategy and mechanism for the evolution of heme redox proteins. The current library approach may provide a test bed for in vitro evolution through subsequent generations of variation, which might more fully explore the range of accessible potential within a fixed topology. Such experiments are in progress now and will be presented in due course.

ACKNOWLEDGMENT

We gratefully acknowledge István Pelczer for assistance with the NMR experiments, Professor Michael Hecht for helpful discussions (and the plasmids pRW1 and pRW2), and George Gallup and Jack Ludwig of Gallup Research for helpful discussions regarding statistical analysis.

REFERENCES

1. Dolla, A., Blanchard, L., Guerlesquin, F., and Bruschi, M. (1994) *Biochimie 76*, 471.
2. Mauk, A. G., and Moore, G. R. (1997) *J. Biol. Inorg. Chem. 2*, 119.
3. Brayer, G. D., and Murphy, M. E. P. (1996) in *Cytochrome c, A Multi-Disciplinary Approach* (Scott, R. A., and Mauk, A. G., Eds.) University Science Books: Sausalito, CA; pp 101−166.
4. Komar-Panicucci, S., Bixler, J., Bakker, G., Sherman, F., and McLendon, G. (1992) *J. Am. Chem. Soc. 114*, 5443.
5. Davies, A. M., Guillemette, G., Smith, M., Greenwood, C., Thurgood, A. G. P., Mauk, A. G., and Moore, G. R. (1993) *Biochemistry 32*, 5431.
6. Cutler, R. L., Davies, A. M., Creighton, S., Warshel, A., Moore, G. R., Smith, M., and Mauk, A. G. (1989) *Biochemistry 28*, 3188.
7. Rafferty, S. P., Pearce, L. L., Barker, P. D., Guillemette, J. G., Kay, C. M., and Smith, M. (1990) *Biohemistry 29*, 9365.
8. Komar-Panicucci, S., Weis, D., Bakker, G., Qiao, T., Sherman, F., and McLendon, G. (1994) *Biochemistry 33*, 10556.
9. Langen, R., Brayer, G. D., Berghuis, A. M., McLendon, G., Sherman, F., and Warshel, A. (1992) *J. Mol. Biol. 224*, 589.
10. Rivera, M., Seetharaman, R., Girdhar, K., Wirtz, M., Zhang, X., Wang, X., and White, S. (1998) *Biochemistry 37*, 1485.
11. Wang, Y.-H., Cui, J., Sun, Y.-L., Yao, P., Zhuang, J.-H., Xie, Y., and Huang, Z.-X. (1997) *J. Electroanal. Chem. 428*, 39.
12. Yao, P., Wang, Y.-H., Xie, Y., and Huang, Z.-X. (1998) *J. Electroanal. Chem. 445*, 197.
13. Hamada, K., Bethge, P. H., and Mathews, F. S. (1995) *J. Mol. Biol. 247*, 947.
14. Arnesano, F., Banci, L., Bertini, I., Faraone-Mennella, J., Rosato, A., Barker, P. D., and Fersht, A. R. (1999) *Biochemistry 38*, 8657.
15. Brunet, A., Huang, E. S., Huffine, M. E., Loeb, J. E., Weltman, R. J., and Hecht, M. H. (1993) *Nature 364*, 355.
16. Kadowaki. H., Kadowaki, T., Wondistord, F. L., and Taylor, S. I. (1989) *Gene 76*, 161.
17. Reidharr-Olsen, J. F., et al. (1991) *Methods Enzymol. 208*, 564.
18. Delaglio, F., Grzesiek, S., Vuister, G. W., Zhu, G., Pfeifer, J., and Bax, A. (1995) *J. Biomol. NMR 6*, 277−293.
19. Johnson, L. A., and Blevins, R. A. (1994) *J. Biomol. NMR 4*, 603.
20. Pelczer, I., and Carter, B. G. (1997) *Methods Mol. Biol. 60*, 71−156.
21. Pelczer, I., and Bishop, K. D. (1997) in *Methods for Structure Elucidation by High-Resolution NMR* (Kover, K. E., Batta, G., and Szantay, C., Jr., Eds.) pp 187−202, Elsevier, New York.
22. Triola, M. (1998) *Elementary Statistics*, Addison-Wesley, Reading, MA.
23. See, for instance: Reidharr-Olsen, J. F., and Sauer, R. T. (1988) *Science 241*, 53.
24. Barker, P. D., Butler, J. L., de Oliveira, P., Hill, H. A. O., and Hunt, N. (1996) *Inorg. Chim. Acta 252*, 71.
25. Moore, G. R., Williams, R. J. P., Peterson, J., Thomson, A. J., and Mathews, F. S. (1985) *Biochim. Biophys. Acta 829*, 83.
26. Churg, A. K., and Warshel, A. (1986) *Biochemistry 25*, 1675.
27. Barker, P. D., Nerou, E. P., Freund, S. M. V., and Fearnley, I. M. (1995) *Biochemistry 34*, 15191.
28. Wu, J.-Z., Mar, G. N. L., Yu, L. P., Lee, K.-B., Walker, F. A., Chiu, M. L., and Sligar, S. G. (1991) *Biochemistry 30*, 2156.
29. Kish, L. (1965) *Survey Sampling*, John Wiley and Sons, Inc., New York.
30. Tezcan, F. Akif, Winkler, J. R., and Gray, H. B. (1998) *J. Am. Chem. Soc. 120*, 13383.

BI0001675